

Inclusive ${}^2\text{H}({}^3\text{He},\text{t})$ reaction at 2 GeV

B. Ramstein¹, C.A. Mosbacher², D. Bachelier^{1,†}, I. Berquist^{3,†}, M. Boivin⁴, J.L. Boyard¹, A. Brockstedt³, L. Carlén³, R. Dahl⁵, P. Ekström³, C. Ellegaard⁵, C. Gaarde^{5,†}, T. Hennino¹, J.C. Jourdain¹, C. Goodman⁶, J.S. Larsen⁵, P. Radvanyi^{1,4}, M. Roy-Stephan¹

¹ Institut de Physique Nucléaire, IN2P3(CNRS), 91406 Orsay Cedex, France

² Institut für Kernphysik, Forschungszentrum Jülich GmbH, 52425 Jülich, Germany

³ Institute of Physics, University of Lund, 223 62 Lund, Sweden

⁴ Laboratoire National Saturne, IN2P3(CNRS) and DSM(CEA), 91191 Gif-sur-Yvette Cedex, France

⁵ Niels Bohr Institute, University of Copenhagen, 2100 Copenhagen, Denmark

⁶ Indiana University, Bloomington, IN 47405, USA

Received: 19 April 1999 / Revised version: 5 July 1999

Communicated by W. Weise

Abstract. The inclusive ${}^2\text{H}({}^3\text{He},\text{t})$ reaction has been studied at 2 GeV for energy transfers up to 500 MeV and scattering angles from 0.25° up to 4° . Data are well reproduced by a model based on a coupled-channel approach for describing the NN and $N\Delta$ systems. The effect of final state interaction is important in the low energy part of the spectra. In the delta region, the cross-section is very sensitive to the effects of Δ -N interaction and $\Delta N \rightarrow NN$ process. The latter has also a large influence well below the pion threshold. The calculation underestimates the experimental cross-section between the quasi-elastic and the delta peaks; this is possibly due to projectile excitation or purely mesonic exchange currents.

PACS. 25.55.Kr ${}^2\text{H}$, ${}^3\text{He}$ - and ${}^4\text{He}$ -induced charge exchange reactions – 14.20.Gk Baryon resonances with $S=0$ – 24.10.Eq Coupled channel and distorted wave models

1 Introduction

The $({}^3\text{He},\text{t})$ reaction at 2 GeV studied at Laboratoire National Saturne in both inclusive [1–3] and exclusive [4,5] experiments on carbon and heavier nuclei has proven to be a very useful tool to investigate the Δ -N interaction [6,7]. In all charge exchange reactions [8–11], the excitation of the Δ resonance involves both a spin longitudinal (pion-like) and a spin transverse (ρ -meson-like or photon-like) coupling, like in pion and photon induced reactions respectively. However, in the case of charge exchange experiments, nuclear response functions are explored in the space-like region ($\omega < q$) that cannot be reached in pion or photon induced experiments.

Microscopic Δ -hole models developed for charge exchange reactions suggest that the response of nuclei to the spin-isospin excitation induced by charge exchange probes is especially sensitive to the spin longitudinal component of the Δ -N interaction, which is strong and attractive at the relevant momentum transfers. This results in a shift of the response towards lower energy transfers, in agreement with the observed peak positions of the Δ resonance in the ${}^{12}\text{C}(p,n)$, ${}^{12}\text{C}({}^3\text{He},\text{t})$ and ${}^{208}\text{Pb}({}^3\text{He},\text{t})$ reactions [12,13]. In addition, the calculations of exit channels are in qualita-

tive agreement with the results of exclusive experiments [14–17]. However, these models are not able to reproduce the whole cross-section in the region of excitation of the Δ resonance and underestimate very much the yield in the so-called dip region lying between the quasi-elastic and the Δ peaks.

A recent analysis within the Δ -hole model of the (p, n) polarisation observables in the Δ region [11] has shown that the underestimate of the cross-section is mainly concentrated in the transverse component of the cross-section, the longitudinal contribution being fairly well reproduced by the model. This last result, together with the successful description of coherent pion production data within the Δ -hole model [15], support the conclusion of attractive Δ -hole correlations in the spin longitudinal channel.

In the quasi-elastic region, a similar result has been obtained [18]. A DWIA calculation with a residual interaction based on a $\pi + \rho + g'$ model is able to reproduce the longitudinal response while the transverse response is underestimated by more than a factor 2.

This excess of experimental cross-section in the transverse channel is of high interest. Roles of 2p-2h correlations and meson-exchange currents are invoked to explain this effect, but more theoretical work is needed to confirm these hypotheses.

[†] deceased

Experimental data on the ${}^2\text{H}$ nucleus can be helpful for understanding the roles of the Δ -N interaction and meson-exchange currents alone. In addition, deuterium is a two-body system with a well-known wave function and the analysis is therefore simpler than for heavier nuclei. Very recently, Ch. Mosbacher and F. Osterfeld [19] proposed a theoretical calculation of the ${}^2\text{H}(\text{p},\text{n})$ reaction based on a coupled channel approach to describe the intermediate Δ -N or NN system in a non-relativistic framework. This model allows a calculation of the energy transfer spectra in the quasi-elastic, dip and Δ regions as well as in the different exit channels ($\pi\text{d}, \pi\text{NN}, \text{NN}$) and has been compared to the LAMPF ${}^2\text{H}(\text{p},\text{n})$ [19] data covering the whole energy transfer range up to 500 MeV and to the ${}^2\text{H}(\mathbf{p}, \mathbf{n})$ data measured in the dip and delta regions [20]. An overall successful description of the total energy transfer spectra is obtained in the quasi-elastic and Δ regions. As in the case of ${}^{12}\text{C}$, the model fails however to describe the dip region and the low energy side of the resonance and this discrepancy again arises from the transverse component. This is interpreted by the authors as an effect of two-body meson-exchange currents and put together with the significant effect of such processes in (e,e') reactions [21].

On the other hand, a small contribution from excitation of a Δ resonance in the projectile is also expected on the low energy side of the Δ and the exact size of this contribution is a subject of investigation [22].

Previous studies of the $({}^3\text{He},\text{t})$ reaction have proven that it behaves at a given four-momentum transfer exactly like the (p,n) reaction except for the $({}^3\text{He},\text{t})$ form factor which produces a much steeper decrease of the cross-section as a function of momentum transfer [2].

No data on spin-observables have been obtained for the ${}^2\text{H}({}^3\text{He},\text{t})$ experiment. However, in addition to inclusive spectra, decay channels have been measured at Laboratoire National Saturne and can possibly bring some constraints on effects of meson exchange currents and projectile excitation, since the former only contributes to the 2p and the latter to the πNN or πd exit channels. It is therefore of high interest to also analyse the ${}^2\text{H}({}^3\text{He},\text{t})$ reaction in the framework of [19].

We focus in this paper on the inclusive ${}^2\text{H}({}^3\text{He},\text{t})$ data at 2 GeV. After a short description of the experimental set-up (Sect. 2), we give our experimental results (Sect. 3), we present the main ingredients of the model (Sect. 4), compare calculations with experimental data (Sect. 5) and give our conclusions (Sect. 6).

2 Experimental set-up

The $({}^3\text{He},\text{t})$ experiment has been performed using a 2 GeV ${}^3\text{He}$ beam delivered by the synchrotron of the Laboratoire National Saturne at Saclay. Outgoing tritons were momentum analysed with the Spes4 spectrometer, a D5Q6S2 instrument 35m long from target to focal plane [23]. The maximum rigidity of this spectrometer was 4 GeV/c and its momentum acceptance was $\Delta p/p \sim 7.10^{-2}$. Angular

acceptance resulted from the combination of the beam emittance of 0.3^0 (FWHM) in the horizontal plane and 1.3^0 (FWHM) in the vertical plane and of the spectrometer front collimator aperture angles of $\pm 0.15^0$ in the horizontal plane and $\pm 0.3^0$ in the vertical plane. As detailed characteristics of the Spes4 spectrometer and its detection system have been given in [23] and [24], we will present only their main features.

The focal plane was equipped with two drift chambers 1m apart in order to ray-trace scattered particles. These 1m wide and 0.2m high chambers consisted of three planes each, two of them with vertical wires and one with wires at 45^0 . The cell size was 5 cm for each plane and the anode wires were arranged in doublets in order to solve the left-right ambiguity. A position resolution of .5 mm (FWHM) was obtained.

The overall resolution on the triton momentum was about 10^{-3} (i.e. 3 MeV at 2 GeV) and was dominated by beam spot size on target. An overall efficiency of about 95% was obtained for the measurement of the tritons.

To cover the quasi-elastic and Δ peaks, tritons with energies between 1.5 and 2 GeV were detected. The whole spectrum was obtained by means of four field settings of the spectrometer. The 70-100 MeV wide overlap regions were in satisfactory agreement.

The data taking was triggered by a coincidence signal between two scintillator hodoscopes situated 16 meters apart. Due to the small momentum acceptance of the spectrometer, only tritons reached the detectors, except at the lowest magnetic fields, where a small deuteron contribution was rejected using a time of flight measurement between the two hodoscope planes.

The ${}^2\text{H}({}^3\text{He},\text{t})$ reaction has been studied at 0.25^0 , 1.6^0 , 2.7^0 and 4.0^0 . The SPES4 spectrometer is not movable and the different scattering angles were achieved with a beam swinger device aimed at changing the angle of the beam impinging on the target. For each measurement, the scattering angle was deduced from the positions of the beam on two insertable wire chambers located in the target area. The residual angular off-set was obtained with a precision of 0.07^0 (rms) by measuring the cross-section of the Gamow-Teller peak in the reaction ${}^{12}\text{C}({}^3\text{He},\text{t}){}^{12}\text{N}_{gs}$ for several angular settings of the spectrometer, both right and left of the beam direction.

The cross-sections on ${}^2\text{H}$ have been obtained by subtraction of the yields obtained on CD2 and C targets. Beam intensities of about 10^9 - 10^{10} particles/s and target thicknesses of 200 mg/cm^2 were used. The average contribution from the carbon nuclei to the CD2 target is about 30 to 45 % depending on the angle. The discrete states of the ${}^{12}\text{C}$ nucleus that show up as narrow peaks in the CD2 spectrum at the smallest angles allow to check the validity of the subtraction with good precision.

As described in [25], the cross-section absolute normalisation was obtained using the known elastic cross-section of ${}^3\text{He}$ on protons. Due to the uncertainties in these cross-sections and in target thicknesses this overall absolute normalisation was determined within 15%.

3 Experimental results

The whole energy transfer distributions obtained in our experiment at four different angles of the spectrometer are displayed on Fig. 1 on a logarithmic scale. Two structures show up very clearly: a quite narrow peak at low energy transfers corresponding to quasi-elastic mechanisms involving only nucleonic degrees of freedom and a broad bump, above the pion threshold, corresponding to the excitation of a nucleon into a Δ resonance. Figs. 2 and 4 show more precisely these two peaks on a linear scale. We have arbitrarily set the dividing line between the two contributions at an energy transfer of 140 MeV, and the respective yields have been integrated and are plotted on Figs. 3 and 5. For each measurement, the distributions of scattering angles accepted by the set-up have been calculated, taking into account beam emittance and collimator aperture. The angles and the horizontal bars reported on the figures correspond respectively to the mean values and the rms of these distributions. The angle mean values are 0.40° , 1.70° , 2.76° and 4.0° when the spectrometer is set at 0.25° , 1.6° , 2.7° and 4° respectively. The rms angular acceptance is about 0.17° for the four settings.

The integrated cross-section of the low energy peak decreases by a factor 11 between 0.25° and 4° as can be seen from the figures 1 to 5 but the most impressive effects

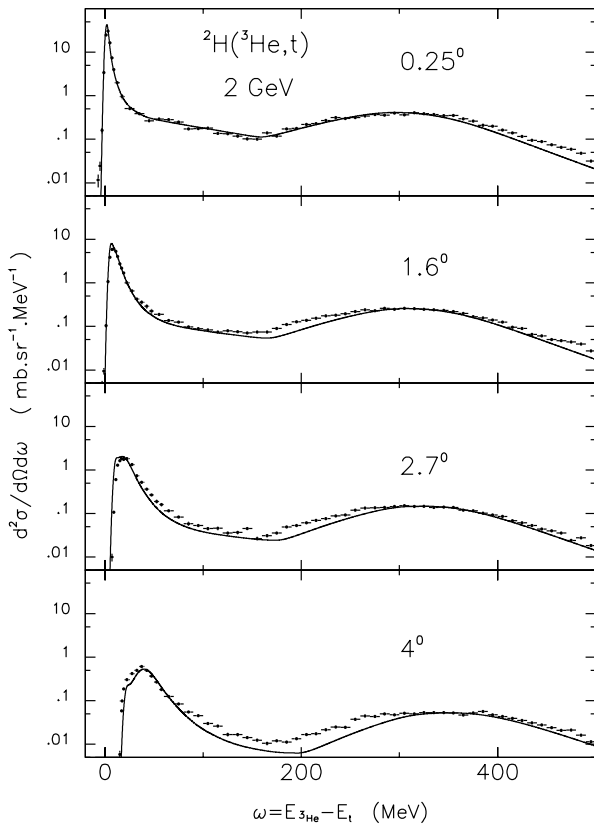


Fig. 1. Energy transfer spectra (full dots) at 4 angles on a logarithmic scale compared to the calculation described in section 4 (full line). The calculations have been folded with the experimental energy resolution and angular acceptance

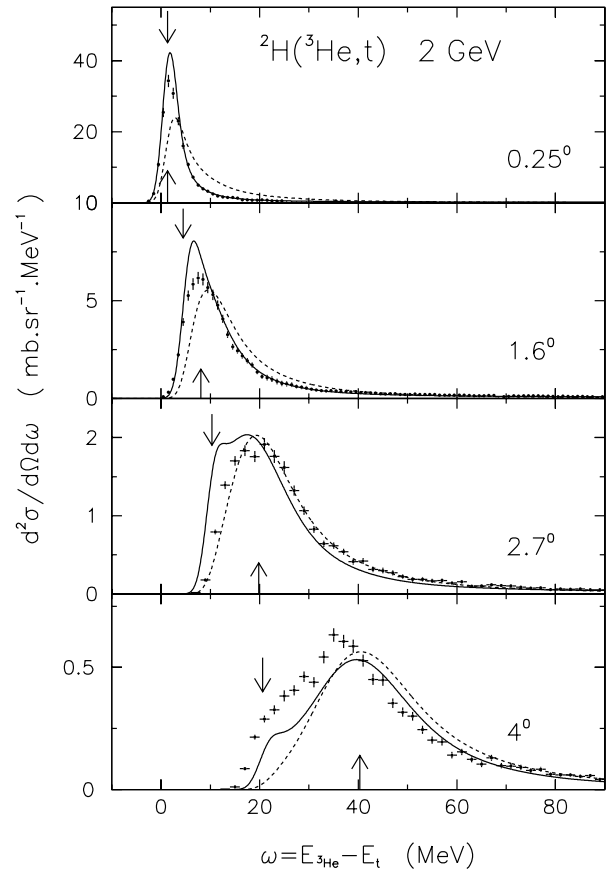


Fig. 2. Energy transfer spectra in the low-energy region (full dots) compared to the full calculation (full line) and to the calculation without FSI (dashed line). The calculations have been folded with the experimental energy resolution and angular acceptance. The upper and lower arrows indicate respectively the energy transfers for kinematics on a 2 proton pair with zero relative momentum and quasi-free kinematics on a nucleon at rest. These values are calculated for the mean angles accepted by the set-up (see text)

are the shift of the peak position and the increase of its width as the angle gets larger. The Δ excitation cross-section has a smoother behaviour as a function of angle since the cross-section only decreases by a factor 7 from 0.25° to 4° and the width stays about constant. However, the position of the maximum shifts by about 45 MeV from 0.25° to 4° .

The presence of these two structures and their different behaviour as a function of angle is a very general feature of all charge exchange reactions [26,9]. For the smallest angles in heavy target nuclei, the low energy peak is due mainly to spin-isospin excitations leading to the ground state, excited states or giant resonances of the resulting $(Z+1, N-1)$ nucleus [25,27]. Quasi-elastic processes corresponding to reactions on a quasi-free nucleon are quenched by Pauli blocking for the smallest momentum transfers but dominate the spectra at larger angles.

For $({}^3\text{He},\text{t})$ on a deuterium nucleus, final state interaction (FSI) will modify the spectrum in the quasi-elastic

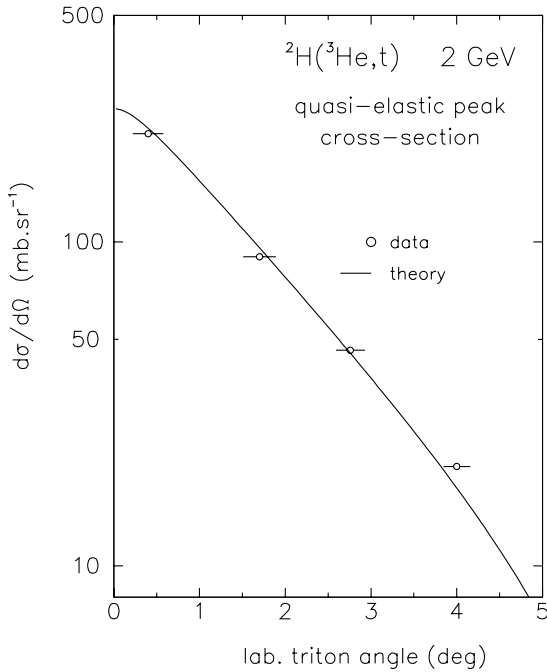


Fig. 3. Angular distribution of the quasi-elastic peak (open circles) compared to the theoretical prediction. The abscissa and the horizontal bar of each data point take into account angular acceptance effects

region. In particular, there is a strong effect of the 1S_0 quasi-bound state for the smallest relative momenta between the 2 protons, (i.e. the smallest momentum transfers). A sizeable effect of this final state interaction in the ${}^2\text{H}(p,n)pp$ reaction at 800 MeV and 1 GeV has been previously found [28–31], so that we can expect this effect to contribute also in the case of the $({}^3\text{He},t)$ reaction. As an indication, energy transfers calculated in quasi-free kinematics and with kinematics corresponding to 2 protons with no relative energy have been indicated on Fig. 2. The energy transfer regions, where the quasi-free and the quasi-bound 1S_0 final state are expected to contribute, separate when the angle increases.

It was shown in [3] that the Δ excitation cross-section in nuclei was following a universal trend as a function of angle. This is also the case for the ${}^2\text{H}$ target as shown on Fig. 5, where the angular distribution on ${}^2\text{H}$ is compared to the ones measured on ${}^1\text{H}$ and ${}^{12}\text{C}$ [3]. It shows that the shape of the angular distribution is mainly dominated by $({}^3\text{He},t)$ form factor effects, whereas the position of the maximum of the Δ resonance depends on the target (see Fig. 6) and is thus sensitive to the presence of other target nucleons.

The Δ peak appears about 25 MeV lower on the ${}^2\text{H}$ target than on ${}^1\text{H}$ at 0.25° . For ${}^{12}\text{C}$ and heavier nuclei, the universal 70 MeV shift towards lower energy with respect to the ${}^1\text{H}$ target has been stressed for a long time. It has been shown that the residual Δ -N interaction was

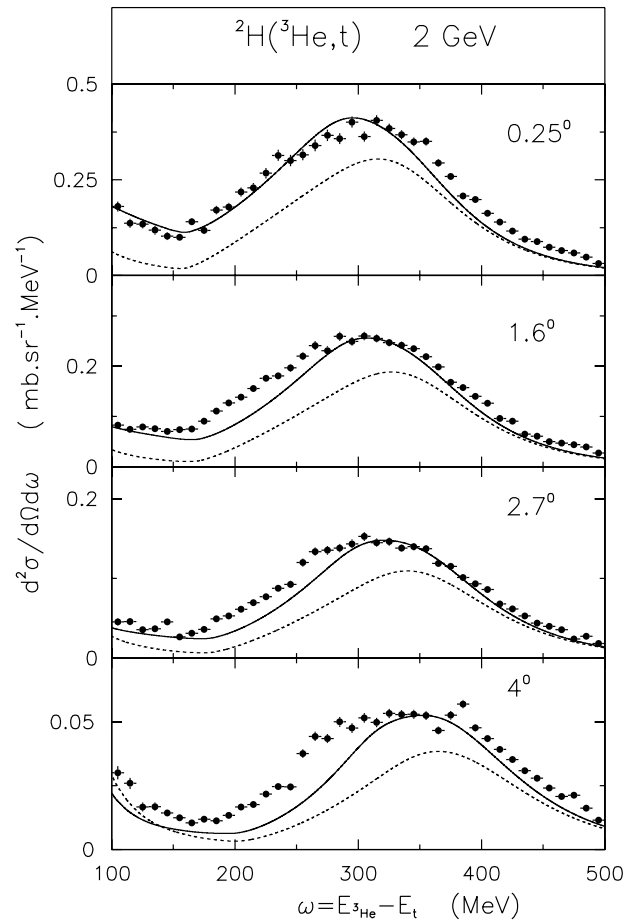


Fig. 4. Energy transfer spectra in the Δ region (full dots) compared to the complete calculation (full line) and to the spectator approximation calculation, i.e. without Δ -N interaction nor $\Delta N \rightarrow NN$ process (dotted line). The calculations have been folded with the experimental energy resolution and angular acceptance

responsible for a 25–30 MeV shift [13,12], the other half being due to more conventional effects, such as the absorption of the Δ resonance ($\Delta N \rightarrow NN$) and the combined effects of Fermi broadening and of the steep $({}^3\text{He},t)$ form factor. In this respect, the specific interest of the deuterium nucleus is to allow a direct study of the effect of the Δ -N interaction, the Fermi motion effects being exactly treated. These suitable properties of the deuterium nucleus have been well exploited in the theoretical interpretation of pion and photon induced reactions [32–38] and in the recent calculation of the ${}^2\text{H}(p,n)$ reaction by Ch. Mosbacher and F. Osterfeld, which we will adapt to describe the $({}^3\text{He},t)$ experiment.

4 Theoretical framework

The model of [19] is most suitable to describe our data, since it allows a description of the charge-exchange reac-

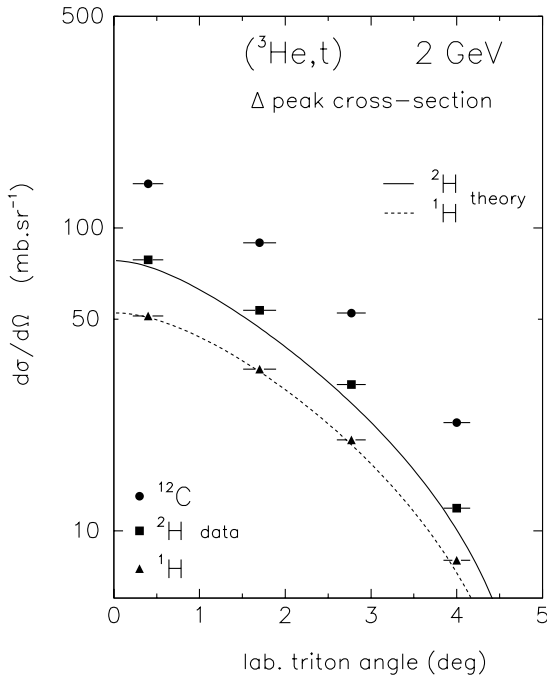


Fig. 5. Angular distribution of the Δ peak for the ${}^2\text{H}({}^3\text{He},t)$ reaction compared to the results of [3] on ${}^1\text{H}$ and ${}^{12}\text{C}$ targets. The abscissa and the horizontal bar of each data point take into account angular acceptance effects. The theoretical predictions for the ${}^2\text{H}$ and ${}^1\text{H}$ nuclei are shown as full and dashed line respectively

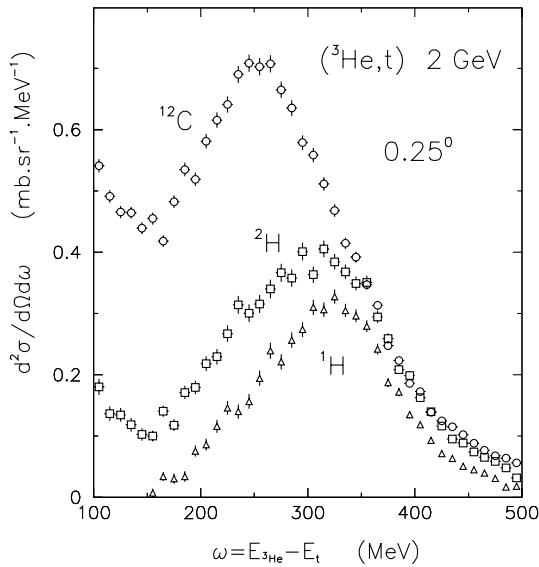


Fig. 6. Energy transfer spectra in the Δ region for the ${}^2\text{H}({}^3\text{He},t)$ reaction compared to the results of ref [3] on ${}^1\text{H}$ and ${}^{12}\text{C}$ nuclei. The calculations have been folded with the experimental energy resolution and angular acceptance

tion in the full energy transfer range covered by our experiment, that means including both quasi-elastic and Δ excitation processes.

The scattering mechanisms considered in the model are represented by the diagrams of Fig. 7. The theoretical framework is based on a coupled channel formalism which allows one to include both the intermediate ΔN interaction and the NN final state interaction in infinite order. The corresponding interaction potentials are constructed in a meson exchange model [39] where π , ρ , ω and σ exchange are taken into account. The Δ resonance is treated thereby as a quasi-particle with a given mass and an intrinsic energy-dependent width. Evaluation of matrix elements involves the propagation of correlated two particle systems, the wave functions of which are calculated in configuration space using the source function formalism and the Lanczos method. For a more detailed explanation, please see [19, 15].

Inputs of the model are the meson and baryon masses, coupling constants, and form factor cutoffs as given in [19] (Table I). All of them are fixed by the ${}^2\text{H}(p,n)$ data and by other sources (such as pion absorption on the deuteron, and NN scattering, e.g.). Furthermore, effective parameterizations of $NN \rightarrow NN$ and $NN \rightarrow N\Delta$ transition matrices are used in order to describe the quasielastic and the Δ excitation in the deuteron caused by projectile.

With respect to the (p,n) reaction, the transition matrices for the $({}^3\text{He},t)$ reaction are modified in two aspects. First, a $({}^3\text{He},t)$ transition form factor has to be applied because of the spatial extension of the projectile-ejectile system. In the present work, we use the form factor of Desgrolard et al. [40], which is based on a three-body Fadeev

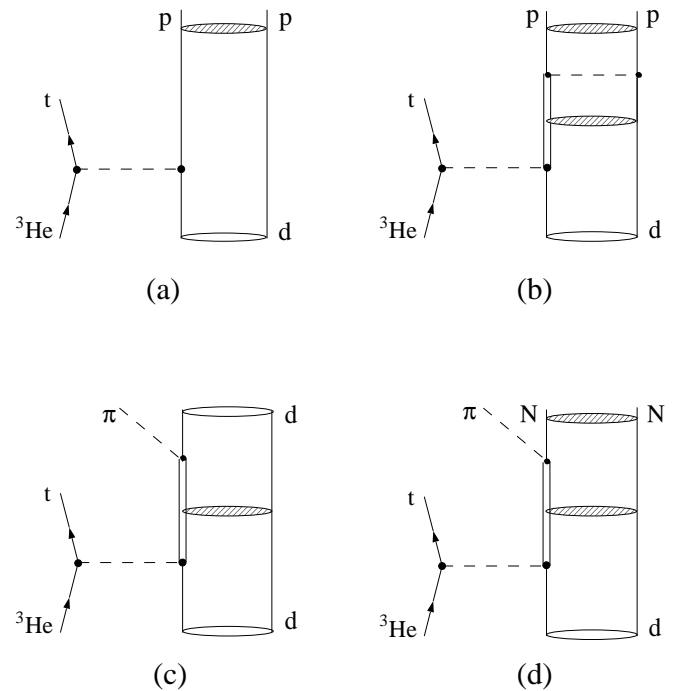


Fig. 7. Feynman diagrams for the reaction mechanisms included in the model of [19]. They represent: (a) quasi-elastic scattering, (b) Δ - $N \rightarrow NN$ process, (c) coherent pion production, (d) quasi-free Δ decay. The shaded areas indicate the intermediate ΔN and NN final state interaction

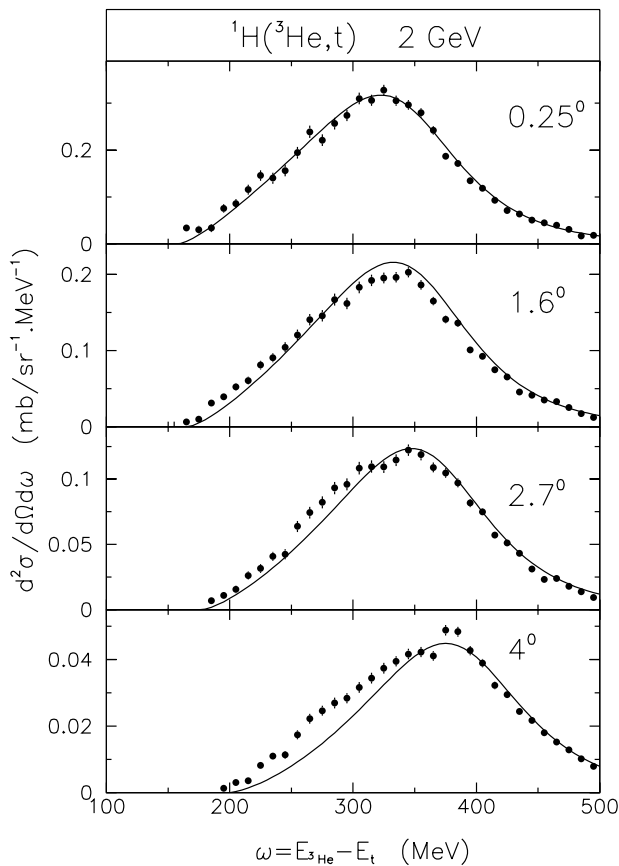


Fig. 8. Comparison of the calculation (full line) with the experimental data in ${}^1\text{H}({}^3\text{He},t)$ reaction at 2 GeV. The calculations have been folded with the experimental energy resolution and angular acceptance

calculation. Second, an additional vertex factor $Z(s_\Delta, t)$ was introduced in order to account for off-shell corrections in the case of the Δ excitation. Here, we follow the arguments of Dmitriev et al. and adopt their specific choice for the $Z(s_\Delta, t)$ vertex factor, see (12) in [41].

With the two modifications mentioned, we achieve a very good description of the ${}^1\text{H}({}^3\text{He},t)\Delta^{++}$ charge exchange reaction at 2 GeV. The quality of the fit is demonstrated in Fig. 8, where experimental ${}^1\text{H}({}^3\text{He},t)$ data are compared to the theoretical cross sections. Obviously, the energy transfer and scattering angle dependence can be both reproduced correctly. As compared to the parameterization given in [15], the different $({}^3\text{He},t)$ transition form factor and the additional vertex factor $Z(s_\Delta, t)$ clearly improve the description at non-zero scattering angles and for low energy transfers, respectively. At the same time, the model preserves full consistency with the (p, n) charge exchange reaction data on the proton as well as on the deuteron target.

5 Discussion

Results of the full calculation described in Sect. 4 are compared to our ${}^2\text{H}({}^3\text{He},t)$ experimental results on Figs. 1 to 5. An overall good agreement is observed for the whole spectrum at the four angles. Both the quasi-elastic and the Δ peak cross-sections are satisfactorily described in shape and magnitude. For the low-energy peak, the very fast evolution of the cross-section with angle is well reproduced by the calculation.

To achieve a consistent comparison with the experimental energy transfer spectra, the calculation has been folded with a gaussian ($\sigma=1.3$ MeV) to account for the experimental energy resolution. This is necessary in the quasi-elastic region for the smallest angles where the theoretical peak is very narrow.

Concerning the effect of angular resolution, we weighted the theoretical angular distribution by the angular transmission of the set-up in order to take into account both collimator aperture and beam emittance in the theoretical spectrum and make the comparison as fair as possible.

A limitation of our experiment arises from the fact that the exact angle of the measurement is known to an overall offset of $\pm 0.07^\circ$ (rms). Since the peak position and width vary as the square of the scattering angle and the slope of the cross-section also increases with angle, the sensitivity of the energy transfer spectra to this offset is the largest at 4° . The biggest effect that can be expected at this angle is a shift of the low energy side and of the peak position of the spectrum by about ± 2 MeV, together with a rescaling of the maximum cross-section of about $\pm 10\%$. The high energy side of the spectrum is insensitive to such variations of angle. Such small effects don't hinder the comparison of the theory to the experiment.

On Fig. 2, we clearly see the important role played by the final state interaction in the model. With respect to the calculation in the spectator approximation, the yield is concentrated at smaller energy transfers. For the largest angles, a shoulder is visible in the theoretical curve at an energy transfer corresponding to small relative momenta of the 2 protons, due to the interaction in the 1S_0 partial wave. The inclusion of 2p final state interaction improves the agreement with experiment at 0.25° , 1.6° and 4° . At 2.7° , the curve without FSI provides a better description of the data, which is not understood so far.

On Figs. 4 and 5, we focus on the Δ region. The description of the data is good especially at the smallest angles. The importance of Δ -N interaction and of the $\Delta N \rightarrow NN$ transition potential is also illustrated on Figs. 5 and 9. The calculation in the spectator approximation, that means neglecting these interactions, underestimates the cross-section and peaks at too high an energy transfer.

The effect of Δ -N interaction has been studied in great detail by Ch. Mosbacher and F. Osterfeld, in the calculation of the ${}^2\text{H}(p,n)$ reaction at 800 MeV covering the same four-momentum transfer regions [19]. They have shown that the shift of the spectrum towards low energy transfers

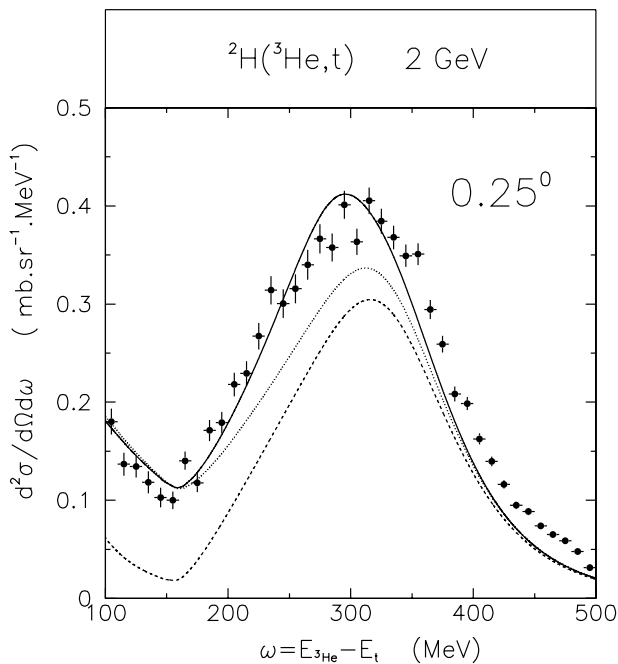


Fig. 9. Energy transfer spectra (full dots) at 0.25° compared to the complete calculation (full line) and to the calculations without Δ -N interaction (dotted line) and in the spectator approximation i.e. without Δ -N interaction nor $\Delta N \rightarrow NN$ process (dashed line)

induced by Δ -N interaction is mainly due to its spin longitudinal part which arises from the pion exchange. This attraction results mainly from the interference between direct and exchange terms. The ρ meson exchange tensor part partly cancels this attraction, but the final result is still a shift of the spectrum towards lower energy transfers.

It is clearly seen on Fig. 9 that the $\Delta N \rightarrow NN$ transition is responsible for a large fraction of the cross-section in the so-called dip region lying between the quasi-elastic and the Δ peaks, but it contributes also to the enhancement and shift of the cross-section in the Δ resonance region.

The cross-section in the dip region and on the low energy side of the resonance is well reproduced at 0.25° but an increasing underestimate by the model is observed as the angle increases. This effect was even worse in the case of the (p,n) reaction and was shown to be due to the transverse contribution of the cross-section, the longitudinal one being well reproduced.

As mentioned in [19], the origin of this deviation may be due to purely mesonic exchange currents, which are not included in the present model. The contribution of these processes in the spin transverse channel has been estimated in the case of the ${}^2\text{H}(\text{p},\text{n})$ reaction at 800 MeV and was found to contribute significantly in the dip region [42, 22].

However, we also observe a small discrepancy on the low energy side of the Δ peak at the higher angles in the case of the reaction on the proton and the question arises whether this could be due either to Δ excitation in

the projectile or to non-resonant pion production, none of which was included in the present calculation. Both contributions are expected mainly on the low energy side of the resonance and projectile excitation is expected to be the more important [43, 22]. Our simulations of the projectile excitation process show a significantly broader angular distribution than in the case of target excitation. These two qualitative arguments favour the interpretation of the residual discrepancy in terms of projectile excitation. Furthermore, the fact that this discrepancy is slightly worse in the case of ${}^2\text{H}$ than in the case of ${}^1\text{H}$ goes also in the right direction. It has indeed been stressed for a long time that the relative weight of the projectile excitation was expected to be enhanced by a factor 3 in the deuterium nucleus with respect to the proton, due to isospin coefficients [43]. However, our analysis shows that the contribution of the projectile excitation to the energy transfer spectrum is quite small and that it is not responsible for the shift observed from ${}^1\text{H}$ to ${}^2\text{H}$ nuclei.

6 Conclusion

We have presented data obtained in the ${}^2\text{H}({}^3\text{He},\text{t})$ reaction at 2 GeV at $0.25^\circ, 1.6^\circ, 2.7^\circ$ and 4° for energy transfers ranging from the quasi-elastic region up to the Δ resonance region.

The analysis is performed in the framework of a model derived from [19] and based on a coupled channel approach to describe the NN and Δ -N systems. This model has been used to calculate the ${}^2\text{H}(\text{p},\text{n})$ reaction at 800 MeV. Taking advantage of the detailed study of the ${}^1\text{H}({}^3\text{He},\text{t})$ reaction, we use in this work a slightly different parametrisation of the Δ resonance [41] excitation process and introduce the $({}^3\text{He},\text{t})$ form factor of [40].

The model reproduces very well the quasi elastic and Δ peaks. The FSI between the 2 protons is shown to modify significantly the spectrum in the low energy region at the smallest angles. In the Δ region, both the $\Delta N \rightarrow NN$ transition and the $\Delta - N$ residual interaction increase and shift the cross-section towards lower energy transfers. The effect of the $\Delta N \rightarrow NN$ transition well below the Δ resonance is also clearly demonstrated. The whole spectrum is very well reproduced for the smallest angle. However, at large angles, an increasing underestimate of the cross-section in the dip region and on the low energy side of the resonance is observed. These small deviations from the model have to be put together with the excess of cross-section observed in the transverse channel in the ${}^2\text{H}(\text{p},\text{n})$ reaction and can possibly be ascribed to projectile excitation or meson exchange currents which are not included in the model.

We plan to extend this work to the analysis of the exclusive ${}^2\text{H}({}^3\text{He},\text{t})$ measurements studied at 2 GeV at Laboratoire National Saturne. Measurements of the decay channels offer a chance to confront the model in a more selective way and possibly to understand the deviations observed in the dip region and on the low energy side of the resonance.

We are very grateful to our colleagues M. Bedjidian, D. Contardo, J.Y. Grossiord, A. Guichard, R. Haroutunian and J.R. Pizzi from Institut de Physique Nucléaire de Lyon for their friendly and fruitful collaboration to the experiment. We thank the staff of Laboratoire National Saturne for having provided a very steady beam and for their effective technical support.

References

1. C. Ellegaard, C. Gaarde, J. S. Larsen, C. Goodman, I. Bergqvist, L. Carlén, P. Ekström, B. Jakobsson, J. Lytkens, M. Bedjidian, M. Chamcham, J. Y. Grossiord, A. Guichard, M. Gusakov, R. Haroutunian, J. R. Pizzi, D. Bachelier, J. L. Boyard, T. Hennino, J. Jourdain, M. Roy-Stephan, M. Boivin, and P. Radvanyi, *Phys. Rev. Lett.* **50**, 1745 (1983)
2. C. Ellegaard, C. Gaarde, J. S. Larsen, V. Dmitriev, O. Sushkov, C. Goodman, I. Bergqvist, A. B. L. Carlén, P. Ekström, M. Bedjidian, D. Contardo, J. Y. Grossiord, A. Guichard, R. Haroutunian, J. R. Pizzi, D. Bachelier, J. L. Boyard, T. Hennino, M. Roy-Stephan, M. Boivin, and P. Radvanyi, *Phys. Lett.* **154B**, 110 (1985)
3. D. Contardo, M. Bedjidian, J. Y. Grossiord, A. Guichard, R. Haroutunian, J. R. Pizzi, C. Ellegaard, C. Gaarde, J. S. Larsen, C. Goodman, I. Bergqvist, A. Brockstedt, L. Carlen, P. Ekström, D. Bachelier, J. L. Boyard, T. Hennino, J. C. Jourdain, M. Roy-Stephan, M. Boivin, and P. Radvanyi, *Phys. Lett.* **168B**, 331 (1986)
4. T. Hennino, B. Ramstein, D. Bachelier, H. G. Bohlen, J. L. Boyard, C. Ellegaard, C. Gaarde, J. Gosset, J. C. Jourdain, J. S. Larsen, M. C. Lemaire, D. L'Hôte, H. P. Morsch, M. Österlund, J. Poitou, P. Radvanyi, M. Roy-Stephan, T. Sams, K. Sneppen, O. Valette, and P. Zupranski, *Phys. Lett.* **283B**, 42 (1992)
5. T. Hennino, B. Ramstein, D. Bachelier, J. L. Boyard, C. Ellegaard, C. Gaarde, J. Gosset, J. C. Jourdain, J. S. Larsen, M. C. Lemaire, D. L'Hôte, H. P. Morsch, M. Österlund, J. Poitou, P. Radvanyi, M. Roy-Stephan, T. Sams, and P. Zupranski, *Phys. Lett.* **303B**, 236 (1993)
6. G. Chanfray and M. Ericson, *Phys. Lett.* **141B**, 163 (1984)
7. V. F. Dmitriev and T. Suzuki, *Nucl. Phys.* **A438**, 697 (1985)
8. M. Roy-Stephan, *Nucl. Phys.* **A488**, 187c (1988)
9. C. Gaarde, *Ann. Rev. of Nuclear and Particle Science* **41**, 187 (1991)
10. D. A. Lind, *Can. J. Phys.* **65**, 637 (1987)
11. D. Prout, S. DeLucia, D. Cooper, B. Luther, E. Sugarbaker, T. Taddeucci, L. J. Rybarczyk, J. Rappaport, B. Park, C. Goodman, G. Edwards, C. Glashauser, T. Sams, T. Udagawa, and F. Osterfeld, *Phys. Rev. Lett.* **76**, 4488 (1996)
12. J. Delorme and P. A. M. Guichon, *Phys. Lett.* **263B**, 157 (1991)
13. T. Udagawa, S. W. Hong, and F. Osterfeld, *Phys. Lett.* **245B**, 1 (1990)
14. P. F. de Cordoba, J. Nieves, E. Oset, and M. Vicente-Vacas, *Phys. Lett* **319B**, 416 (1993)
15. T. Udagawa, P. Oltmanns, F. Osterfeld, and S. Hong, *Phys. Rev. C* **49**, 3162 (1994)
16. B. Körfgen and F. Osterfeld and T. Udagawa, *Phys. Rev.* **C50**, 1637 (1994)
17. M. A. Kagarlis and V. F. Dmitriev, *Phys. Lett.* **408B**, 12 (1997)
18. T. Taddeucci, B. Luther, L. J. Rybarczyk, R. Byrd, J. McClelland, D. Prout, S. DeLucia, D. Cooper, D. Marchlenski, E. Sugarbaker, B. Park, T. Sams, C. Goodman, J. Rappaport, M. Ichimura, and K. Kawahigashi, *Phys. Rev. Lett.* **73**, 3516 (1994)
19. C. Mosbacher and F. Osterfeld, *Phys. Rev. C* **56**, 2014 (1997)
20. D. Prout, S. DeLucia, E. Sugarbaker, B. Luther, D. Cooper, T. Taddeucci, J. McClelland, C. Goodman, B. Park, J. Rappaport, T. Sams, G. Edwards, and C. Glashauser, *Nucl. Phys.* **A577**, 233c (1994)
21. S. Boffi, C. Giusti, and F. D. Pacati, *Phys. Rep.* **226**, 1 (1993)
22. Y. Jo and C. Y. Lee, *Phys. Rev. C* **54**, 952 (1996)
23. E. Grorud, J. L. Laclare, A. Ropert, A. Tkatchenko, J. Banaigs, and M. Boivin, *Nucl. Instr. and Meth.* **A188**, 549 (1981)
24. M. Bedjidian, D. Contardo, E. Descroix, S. Gardien, J. Y. Grossiord, A. Guichard, M. Gusakov, R. Haroutunian, M. Jacquin, J. R. Pizzi, D. Bachelier, J. L. Boyard, T. Hennino, J. C. Jourdain, M. Roy-Stephan, and P. Radvanyi, *Nucl. Instr. and Meth.* **A257**, 132 (1987)
25. I. Bergqvist, A. Brockstedt, L. Carlén, P. Ekström, B. Jakobsson, C. Ellegaard, C. Gaarde, J. S. Larsen, C. Goodman, M. Bedjidian, D. Contardo, J. Y. Grossiord, A. Guichard, R. Haroutunian, J. R. Pizzi, D. Bachelier, J. L. Boyard, T. Hennino, J. C. Jourdain, M. Roy-Stephan, M. Boivin, and P. Radvanyi, *Nucl. Phys.* **A469**, 648 (1987)
26. C. Ellegaard, C. Gaarde, T. S. Jørgensen, J. S. Larsen, C. Goodman, I. Bergqvist, A. Brockstedt, P. Ekström, M. Bedjidian, D. Contardo, J. Y. Grossiord, A. Guichard, D. Bachelier, J. L. Boyard, T. Hennino, J. C. Jourdain, M. Roy-Stephan, P. Radvanyi, and J. Tinsley, *Phys. Rev. Lett.* **59**, 974 (1987)
27. A. Brockstedt, I. Bergqvist, L. Carlén, P. Ekström, B. Jakobsson, C. Ellegaard, C. Gaarde, J. S. Larsen, C. Goodman, M. Bedjidian, D. Contardo, J. Y. Grossiord, A. Guichard, J. R. Pizzi, D. Bachelier, J. L. Boyard, T. Hennino, J. C. Jourdain, M. Roy-Stephan, M. Boivin, T. Hasegawa, and P. Radvanyi, *Nucl. Phys.* **A530**, 571 (1991)
28. B. S. Aladashvili, J. F. Germond, V. V. Glagolev, M. Nioradze, T. Siemiarczuk, J. Stepaniak, V. N. Streltsov, C. Wilkin, and P. Zielinski, *J. Phys. G: Nucl Phys.* **3**, 1225 (1977)
29. H. Sakai, T. A. Carey, J. B. McClelland, T. N. Taddeucci, R. C. Byrd, C. D. Goodman, D. Krofcheck, L. J. Rybarczyk, E. Sugarbaker, A. J. Wagner, and J. Rappaport, *Phys. Rev.* **C35**, 344 (1987)
30. A. Deloff and T. Siemiarczuk, *Nucl. Phys.* **A555**, 659 (1993)
31. A. Itabashi, K. Aizawa, and M. Ichimura, *Prog. of Theor. Phys.* **91**, 69 (1994)
32. O. Maxwell, W. Weise, and M. Brack, *Nucl. Phys.* **A348**, 388 (1980)
33. J. A. Niskanen and P. Wilhelm, *Phys. Lett.* **359B**, 359 (1995)
34. P. Wilhelm and H. Arenhövel, *Nucl. Phys.* **A609**, 469 (1996)

35. S. S. Kamalov, L. Tiator, and C. Bennhold, Phys. Rev. C **55**, 88 (1997)
36. M. Peña, H. Garcilazo, U. Oelke, and P. Sauer, Phys. Rev. C **45**, 1487 (1992).
37. T. Ericson and W. Weise, *Pions and Nuclei* (Clarendon, Oxford, 1988)
38. H. Garcilazo and T. Mizutani, *πNN systems* (World Scientific, Singapore, 1990)
39. R. Machleidt, K. Holinde, and C. Elster, Phys. Rep. **149**, 1 (1987)
40. P. Desgrolard, J. Delorme, and C. Gignoux, Nucl. Phys. **A544**, 811 (1992)
41. V. F. Dmitriev, O. Sushkov, and C. Gaarde, Nucl. Phys. **A459**, 503 (1986)
42. C. A. Mosbacher, Hadronische Reaktionen am Deuteron im Δ -Resonanzbereich, Thesis, Institut für Kernphysik, Forschungszentrum Jülich, Friedrich-Wilhelms-Universität Bonn, 1998
43. E. Oset, E. Shiino, and H. Toki, Phys. Lett. **224B**, 249 (1989)